Article

Not peer-reviewed version

IOC-Aligned Screening of Virgin Olive Oils via Digital Olfaction: Classification and Estimation of Sunflower-Oil Adulteration

Ramiro Sánchez *, Fernando Díaz, Lina Melo

Posted Date: 23 September 2025

doi: 10.20944/preprints202509.1945.v1

Keywords: electronic noise; virgin olive oil; sunflower-oil adulteration; screening

Preprints.org (www.preprints.org) | NOT PEER-REVIEWED | Posted: 23 September 2025 doi:10.20944/preprints202509.1945.v1

Article

IOC-Aligned Screening of Virgin Olive Oils via Digital Olfaction: Classification and Estimation of Sunflower-Oil Adulteration

Ramiro Sánchez [1,*], Fernando Díaz [2] and Lina Melo [3]

[1] Technological Institute of Food and Agriculture (CICYTEX-INTAEX), Junta of Extremadura, Avda. Adolfo Suárez s/n, 06007 Badajoz, Spain
[2] Industrial Engineering School, University of Extremadura, 06006 Badajoz, Spain
[3] Department of Experimental Science and Mathematics Teaching Area, University of Extremadura, 06006 Badajoz, Spain
* Correspondence: ramiro.sanchez@juntaex.es; +34-924-012-656

Abstract

Extra virgin olive oil (EVOO) can degrade during production or storage to virgin olive oil (VOO) or lampante olive oil (LOO). Fraud can also occur during commercialisation through adulteration of EVOO (Ad-EVOO) with cheaper sunflower oil (SFO). Therefore, rapid screening techniques for quality control are needed. We evaluated an electronic nose (EN) with chemometrics—linear discriminant analysis (LDA), artificial neural-network discriminant analysis (ANN-DA), and partial least-squares regression (PLS)—in two scenarios: (i) classification into four classes (EVOO, VOO, LOO, and Ad-EVOO adulterated with 25% w/w SFO); and (ii) Ad-EVOO series containing 5–40% w/w SFO. Classes were corroborated by HS-SPME-GC-MS, with elevated (E)-2-hexenal and 3-hexen-1-ol in EVOO and increases in nonanal, ethyl acetate, and 2-propanol in deteriorated oils. Using the EN, LDA separated the classes, and ANN-DA achieved 90% accuracy under cross-validation, with the greatest confusion between VOO and LOO. In adulteration, discrimination emerged from 20% SFO, and PLS estimated %Ad-EVOO with R^2pred = 0.972 (RMSEC/RMSEP = 8.059/5.627). In conclusion, the EN provides objective, rapid, and non-destructive screening that supports sensory panels and chromatographic analyses during reception and storage in industrial settings.

Keywords: electronic noise; virgin olive oil; sunflower-oil adulteration; screening.

1. Introduction

Virgin olive oil (VOO) is a strategic product in the Mediterranean diet and in the European agri-food economy. Its commercial classification and protection against fraud are structured, at the regulatory level, around the International Olive Council (IOC) panel test for verification of category and sensory defects [1], in coherence with the European Union framework on marketing standards and official controls [2]. The organoleptic classification of virgin oils is based on the median of defect (Md)—the most intense defect in olfactory–gustatory perception—and the median of fruitiness (Mf) [1,2]. In this work, the electronic nose (EN) records volatile compounds exclusively and therefore primarily models the olfactory–retronasal dimension underlying Md and Mf, rather than gustatory or trigeminal sensations. At the mill, there is a need for rapid, non-destructive instrumental screening methods that allow classification of samples during processing, storage, and commercial operations, and that support real-time decision-making without replacing the official organoleptic assessment.

From a chemical standpoint, the aroma of VOO is largely explained by its fraction of volatile organic compounds (VOCs). C6 aldehydes and alcohols from the lipoxygenase pathway are associated with positive attributes (green/ripe fruitiness), whereas oxidative evolution and certain fermentative processes increase saturated aldehydes (e.g., hexanal, nonanal), light acids, and esters,

doi:10.20944/preprints202509.1945.v1

which correlate with sensory defects during storage [3,4]. In this context, the HS-SPME-GC–MS determination of volatiles has been harmonised and interlaboratory-validated as chemical support to sensory classification, with a minimum set of diagnostic molecules associated with the main defects (fusty–muddy sediment, musty–humid–earthy, winey–vinegary, rancid) and with positive attributes [5]. Complementarily, HS-GC–IMS has shown an ability to pre-classify qualities and categories, suggesting its use as a screening tool prior to the panel [6,7].

In parallel, digital olfaction using electronic noses (ENs) with metal-oxide semiconductor (MOS) sensors and chemometric modelling has become established as a rapid, non-destructive, low-cost alternative for food screening and adulteration detection [8]. In olive oil, there is robust prior work demonstrating the detection of blends with seed oils (e.g., sunflower, rapeseed) using ENs and associated chromatographic techniques [9,10], supporting their role as an instrumental filter to flag suspect samples and to optimise the prioritisation of confirmatory analyses. Moreover, the MOS sensors of the device used in this study have performed well in complex matrices (detection of TCA in sparkling wines, olfactory monitoring of sourdough fermentations, and evaluation of specialty coffees), which supports their transferability to industrial oil quality-control scenarios [11–13].

Even with their regulatory and training value, the literature discusses inter-panel reproducibility, alignment, and reference materials for training and quality control of sensory panels, proposing alignment schemes, alternative performance metrics, and certification of stable reference oils [14–16]. In parallel, instrumental screening techniques (HS-GC–IMS, MOS-based ENs) are advancing with robust models and cross/external validations, but they still face challenges in domain of applicability (cultivars, harvests, storage matrices), drift and periodic calibration, as well as the need for interlaboratory validations and guidelines for integration with the panel to avoid false positives/negatives in commercial decisions [16–18]. In any case, there is consensus that these methods should be positioned as objective, traceable support to the panel—rather than substitutes—especially for pre-screening of large lots.

We hypothesise that a MOS-EN, combined with supervised models (LDA/ANN-DA) and PLS regression, could (i) discriminate frequent quality states at the mill and during storage and (ii) estimate VOO–sunflower adulteration within technologically relevant ranges. The aim is to evaluate the EN's capability as a screening method that complements—without replacing—the IOC panel test and chromatographic confirmation (HS-SPME-GC–MS), providing short response times and objective traceability [1,5–7].

2. Materials and Methods

2.1. Samples and Experimental Design

Samples were provided by an olive-oil company in Extremadura, Spain (Compañía Oleícola Siglo XXI S.L – La Chinata). Two sample sets were used:

1. Oils covering different quality categories: extra virgin olive oil (EVOO) corresponding to fresh oil produced in the same year; virgin olive oil (VOO), corresponding to an EVOO stored for 3 years; lampante olive oil (LOO) obtained from a fresh EVOO that deteriorated; and adulterated EVOO (Ad-EVOO; 25% w/w sunflower oil, SFO); total of 80 oils (n = 20 per class). Each sample was measured with the electronic nose (EN), and a chromatographic profile for each class was obtained by HS-SPME-GC–MS according to the IOC harmonised method [1,6].
2. EVOO adulterated with SFO at 5, 10, 20, and 40% (w/w); n = 10 per level.

EN measurements were performed at 28 °C to favour VOC release and in line with the sensory/analytical practice reported for organoleptic analysis of olive oils [1]. The measurement order was randomised by batch and class; blanks and controls were interspersed.

2.2. MOS-EN Device and Data Acquisition

A portable MOS-array EN, shown in Figure 1, was used. It is equipped with an internal pump to draw the headspace from the sealed sample container and a valve that switches between the filtered-air inlet (blank/conditioning) and the sample headspace. Acquisition and control of the measurement cycle (valve switching, exposure and purge times) are handled via a Bluetooth wireless

Preprints.org (www.preprints.org) | NOT PEER-REVIEWED | Posted: 23 September 2025 doi:10.20944/preprints202509.1945.v1

connection to a mobile application. This prototype has previously been used for wine quality control and for monitoring the olfactory evolution of sourdough, as described in earlier studies [12,13].

Figure 1. Prototype electronic nose equipped with MOS sensors.

The board integrates the commercial sensors BME680 (Bosch Sensortec GmbH, Reutlingen, Germany), SGP30 (Sensirion AG, Stäfa, Switzerland), ZMOD4410 (Renesas Electronics Corp., Tokyo, Japan), CCS811 (ams OSRAM AG, Premstätten, Austria), and iAQ-Core (ams AG, Premstätten, Austria).

Each sample was analysed using a cycle of 60 s of air (conditioning) + 60 s of exposure to the sample headspace at 28 °C. Between samples, filtered-air purges (activated carbon) were applied to stabilise the baseline. The sampling setup consisted of a sealed glass vessel with two ports (filtered-air inlet and headspace outlet to the EN); the sample mass was 15 mL as the operational standard.

2.3. HS-SPME-GC–MS Analysis of Volatile Compounds

A representative subset of set (i) was used for corroboration. Aliquots of 5.0 g of oil were placed in 20 mL vials (PTFE/silicone septum); pre-incubation was 5 min at 37 °C; extraction used a DVB/CAR/PDMS 50/30 μm fibre (Supelco, Bellefonte, PA, USA) for 30 min at 37 °C with agitation; desorption was at 200 °C for 5 min in splitless mode.

GC: VF-5 ms column, 30 m × 0.25 mm × 0.25 μm (Agilent J&W, Santa Clara, CA, USA); oven programme 70 → 240 °C at 4 $°C \cdot min^{-1}$; He at 1.0 $mL \cdot min^{-1}$. MS: EI 70 eV, full-scan acquisition (m/z 30–550).

Compound identification relied on matching to the NIST/EPA/NIH library (Gaithersburg, MD, USA) and verification of retention behaviour; accordingly, the reported VOCs should be considered tentative identifications, as analytical standards were not used for confirmation. Peak areas were expressed as relative percentages (normalised to the total volatiles of each chromatogram), thus reflecting headspace composition rather than absolute concentrations. This approach is fit for purpose because the EN responds to the overall volatile profile and to the relative abundances of compounds in the headspace. Target families included C6-LOX volatiles (positive attributes) and oxidation/fermentation markers reported in the literature [5–7].

2.4. Data Analysis

For the classification and interpretation of the EN data, multivariate analysis methods were applied using PLS_Toolbox 9.5 (Eigenvector Research Inc., Wenatchee, WA, USA) within the MATLAB R2024b environment (The MathWorks Inc., Natick, MA, USA).

From the raw EN sensor signals, characteristic values were extracted based on the difference between the maximum value (Xmax)—calculated as the mean of the last five points during exposure to the reference gas (clean air)—and the minimum value (Xmin)—the mean of the last five points during exposure to the sample headspace—defining ΔX = Xmax − Xmin. The data were then autoscaled (mean-centred and scaled to unit variance) to equalise the weight of all variables and improve comparability across sensors. These preprocessing strategies, combined with a controlled measurement environment (28 °C) and the use of clean-air baselines before each reading, help minimise short- and long-term drift and reduce the impact of environmental variability on multivariate interpretation [12,13].

LDA was used for projection/visualisation of the multiclass separation of samples from sets (i) and (ii). LDA is a supervised dimensionality-reduction technique that maximises between-class separation via linear combinations of variables, using a priori labels [7,8].

Subsequently, supervised classification by artificial neural-network discriminant analysis (ANN-DA) was performed on sets (i) and (ii), with cross-validation. To evaluate model performance, metrics derived from the class-wise confusion matrix were computed, giving equal weight to each class (macro-averaging):

- TPR/Recall (sensitivity) = TP/(TP + FN): proportion of class-c samples correctly identified.
- Precision (P) = TP/(TP + FP): fraction of predictions as class c that truly belong to c.
- F1 = 2·(P·Recall)/(P + Recall): harmonic mean balancing precision and recall.

Where TP is the number of true positives, FP the number of false positives, and FN the number of false negatives.

The input variables to LDA and ANN-DA were the ΔX features (and, where appropriate, the pulse slope) per sensor, obtained from resistance/gas-index channels and IAQ-type signals (e.g., TVOC, CO_2eq), following the criterion used in previous work with the same EN [12,13].

For regression on set (ii) (Ad-EVOO series), PLS was used with an 80/20 split for training/external validation stratified by blend level. We report R^2cal, R^2pred, RMSEC, and RMSEP; selection of the number of latent variables (LVs) followed good chemometric practice [18–20].

Chromatographic data processing. Chromatograms/spectra were processed with the instrument software; identification was based on NIST library search and consistency within chemical families. For class comparisons in set (i), one-way ANOVA was applied to peak areas. Tukey's HSD was used for multiple comparisons (α = 0.05). Classical statistical analyses were conducted in IBM SPSS Statistics 20 (IBM Corp., Armonk, NY, USA), in line with our previous approach [12].

3. Results and Discussion

We present olfactory classification with the EN among EVOO, VOO, LOO, and Ad-EVOO (25% w/w SFO); chemical corroboration by HS-SPME-GC–MS that explains this separation; and the detection and quantification of EVOO–SFO adulteration using LDA/ANN-DA and PLS. The practical aim is to evaluate the EN as a rapid, non-destructive screening tool that prioritises official confirmations (panel/GC–MS) at reception and during storage.

3.1. Electronic Nose Screening: Multiclass Classification

Figure 2 shows the LDA projection (LV1 = 90.14%; LV2 = 9.55%).

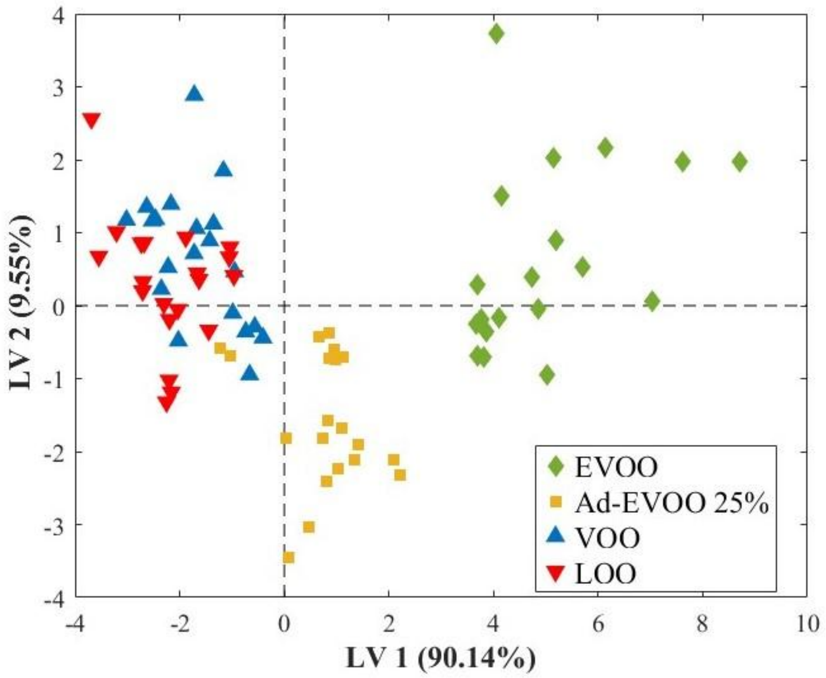

Figure 2. Proyección LDA de EVOO, Ad-EVOO 25%, VOO y LOO.

In Figure 2, EVOO is displaced towards positive LV1 scores (≈4–8), whereas VOO/LOO lie at negative LV1 scores (≈−3 to 0), where a partial overlap appears between VOO and LOO—consistent with the proximity of their volatile signatures as C6-LOX "positive" compounds decline and oxidation/fermentation markers increase. Ad-EVOO 25% occupies an intermediate position (LV1 ≈ 1–3), as expected for a mixed profile without olfactory defects. This pattern—a well-separated "premium" class with a diffuse boundary between lower categories—is typical of recent EN studies on oils and reflects the underlying chemical transition across quality states [15,21].

Applying ANN-DA yielded the confusion matrix shown in Table 1.

Table 1. Confusion matrix of the ANN-DA model under cross-validation.

	Predicted Values			
Actual Values	**EVOO**	**Ad-EVOO 25%**	**VOO**	**LOO**
EVOO	20	0	0	0
Ad-EVOO 25%	0	20	0	0
VOO	0	0	14	2
LOO	0	0	6	18

Table 1 (confusion matrix, cross-validation) shows 90% accuracy, with errors concentrated at the VOO–LOO boundary. The EN discriminates four operational states with 90% accuracy (72/80); the main errors cluster at the aged (VOO) and lampante (LOO) boundary, consistent with their volatile similarity, supporting the usefulness of screening to pre-classify lots at the mill. Table 2 summarises the results after applying the per-class Precision/TPR/F1 metrics.

Table 2. Per-class metrics of the ANN-DA model under cross-validation.

Class	Precision (P)	Sensitivity	F1-score
EVOO	1.00	1.00	1.00
Ad- EVOO 25%	1.00	1.00	1.00
VOO	0.87	0.70	0.77
LOO	0.81	0.90	0.85

In EVOO and Ad-EVOO 25%, F1 = 1.00, implying the absence of both false positives and false negatives for these classes under the employed validation. For VOO and LOO, F1 ≈ 0.78–0.86—a decrease attributable to cross-class confusions between contiguous categories (the VOO↔LOO boundary)—fully consistent with the overlap observed in Figure 2 (LDA projection) and with the errors localised in Table 1 (confusion matrix). In terms of Type I/Type II errors, these figures indicate a reasonable balance between false positives (Type I) and false negatives (Type II) per class: high sensitivity for detecting EVOO and 25% adulterated oil, and greater ambiguity across the VOO–LOO transition. This pattern is expected in tasks with quality gradients and aligns with recent results in which electronic noses coupled to machine learning (ML)—including neural classifiers and other supervised models—separate EVOO from non-EVOO with high sensitivity, while most errors concentrate at the VOO–LOO boundaries due to their chemical and sensory proximity [22,23].

3.2. Chemical Corroboration by HS-SPME-GC–MS

Table 3 shows the chromatographic volatile profile of the three virgin-oil categories and the adulterated sample studied.

Table 3. Volatiles (CAS, TR, odour descriptor) and mean ± SD per class for n = 3 (EVOO, Ad-EVOO, VOO, and LOO). Different lowercase letters indicate significant differences for each volatile across classes (Tukey's test, $p < 0.05$).

				Peak Area (%)			
CAS Number	**Volatile Compound**	**TR**	**Odor Descriptors**	**EVOO**	**Ad-EVOO**	**VOO**	**LOO**
4395-73-7	2-Formylhistamine	1.651	Not well documented	1.54 ± 0.20^{a}	0.96 ± 0.40^{a}	1.41 ± 0.32^{a}	0.1 ± 0.1^{b}
108-24-7	Acetic anhydride	1.751	Pungent, vinegar-like, irritating	0.63 ± 0.26^{c}	2.08 ± 0.36^{b}	3.20 ± 0.37^{a}	2.18 ± 0.36^{b}
540-88-5	1-methoxy-2-propanol	1.914	Alcoholic, slightly sweet, solvent-like	0.11 ± 0.19^{c}	3.03 ± 0.33^{b}	5.64 ± 0.27^{a}	2.77 ± 0.32^{b}
141-78-6	ethyl acetate	2.684	Sweet, fruity, pear-like	0.43 ± 0.75^{c}	8.23 ± 0.41^{b}	0.99 ± 0.17^{c}	9.18 ± 0.33^{a}
96-22-0	3-Pentanone	4.447	Fruity, ethereal, slightly minty	0.92 ± 0.33^{a}	0.67 ± 0.44^{a}	0.84 ± 0.25^{a}	0.89 ± 0.29^{a}
4748-78-1	Hexane, 2,4-dimethyl-	8.88	Gasoline-like, slightly sweet	0.16 ± 0.28^{b}	2.00 ± 0.34^{a}	2.44 ± 0.22^{a}	2.31 ± 0.30^{a}
66-25-1	Hexanal	8.993	Green, grassy, fatty, citrus-like	4.51 ± 0.20^{c}	4.27 ± 0.22^{c}	9.68 ± 0.39^{a}	7.19 ± 0.38^{b}
47-07-03	Hexane, 1-methoxy-	11.251	Ether-like, mildly fruity	0.10 ± 0.18^{b}	0.61 ± 0.32^{b}	1.42 ± 0.43^{a}	0.57 ± 0.21^{b}
6728-26-3	(E)-2-hexenal	13.078	Green, grassy, fresh	10.93 ± 0.23^{a}	9.85 ± 0.39^{b}	3.92 ± 0.20^{c}	9.86 ± 0.36^{b}
928-96-1	3-Hexen-1-ol. (Z)-	13.324	Green, fresh, leafy, cut grass scent	23.00 ± 0.18^{a}	14.88 ± 0.27^{c}	20.17 ± 0.34^{b}	14.81 ± 0.31^{c}
928-94-9	2-Hexen-1-ol. (Z)-	14.063	Green, fresh, slightly sweet	12.98 ± 0.29^{a}	9.09 ± 0.23^{b}	3.98 ± 0.32^{c}	8.74 ± 0.26^{b}
1565-71-5	(S)-3.4-Dimethylpentanol	14.36	Not well documented	10.09 ± 0.31^{a}	10.98 ± 0.43^{a}	8.60 ± 0.32^{b}	10.53 ± 0.32^{a}
123-92-2	isoamyl acetate	14.808	Banana, fruity, sweet	0.15 ± 0.26^{ab}	0.28 ± 0.28^{ab}	0.77 ± 0.27^{a}	0.8 ± 0.14^{b}
111-71-7	Heptanal	16.179	Fatty, citrusy, green, slightly fruity	0.34 ± 0.37^{a}	0.27 ± 0.23^{a}	0.34 ± 0.25^{a}	0.34 ± 0.37^{a}
1838-79-1	3-Ethyl-1.5-octadiene	18.288	Floral, citrus-like	1.47 ± 0.41^{a}	0.75 ± 0.25^{b}	0.77 ± 0.24^{b}	0.79 ± 0.21^{b}

18829-55-5	2-Heptenal. (Z)-	19.32	Fatty, green, herbal	0.28 ± 0.31^{a}	0.48 ± 0.28^{a}	1.05 ± 0.39^{a}	0.59 ± 0.36^{a}
698-10-2	2(5H)-Furanone, 5-ethyl-	19.613	Sweet, caramel-like, slightly burnt	8.43 ± 0.24^{a}	0.82 ± 0.22^{b}	0.79 ± 0.34^{b}	0.78 ± 0.29^{b}
108-95-2	Phenol	20.385	Medicinal, smoky, tar-like	0.13 ± 0.02^{c}	0.76 ± 0.29^{ab}	0.23 ± 0.05^{bc}	0.90 ± 0.20^{a}
18829-56-6	2.4-Heptadienal. (E.E)-	21.288	Fatty, green, waxy	1.91 ± 0.39^{a}	1.92 ± 0.23^{a}	2.11 ± 0.21^{a}	2.17 ± 0.26^{a}
124-13-0	octanal	21.522	Fatty, citrusy, orange-like	0.20 ± 0.28^{a}	0.22 ± 0.21^{a}	0.22 ± 0.20^{a}	0.25 ± 0.18^{a}
32797-50-5	Hexenol acetate	21.55	Green, fruity, apple-like	3.82 ± 0.12^{d}	11.17 ± 0.24^{b}	8.70 ± 0.15^{c}	12.35 ± 0.27^{a}
142-92-7	Hexyl acetate	21.939	Fruity, apple, banana	6.04 ± 0.22^{a}	2.10 ± 0.34^{c}	4.72 ± 0.18^{b}	2.16 ± 0.40^{c}
100-51-6	Benzyl alcohol	23.042	Floral, slightly sweet, almond-like	0.51 ± 0.37^{a}	0.58 ± 0.32^{a}	0.59 ± 0.28^{a}	0.61 ± 0.21^{a}
3779-61-1	(E)-β-ocimene	23.364	Sweet, citrusy, floral	0.89 ± 0.36^{c}	2.20 ± 0.24^{b}	4.92 ± 0.34^{a}	2.34 ± 0.44^{b}
150-76-5	Phenol, 4-methoxy-	25.12	Anisic, sweet, medicinal	0.23 ± 0.32^{b}	1.61 ± 0.31^{a}	0.37 ± 0.24^{b}	1.45 ± 0.22^{a}
93-58-3	Methyl benzoate	25.54	Floral, fruity, slightly minty	0.10 ± 0.11^{a}	0.33 ± 0.20^{a}	0.49 ± 0.38^{a}	0.29 ± 0.30^{a}
124-19-6	Nonanal	25.953	Waxy, citrusy, floral	2.15 ± 0.31^{b}	2.50 ± 0.38^{b}	4.04 ± 0.13^{a}	2.70 ± 0.43^{b}
60-12-8	Phenylethyl Alcohol	26.374	Rose-like, floral, honey	1.69 ± 0.30^{b}	2.55 ± 0.26^{a}	2.16 ± 0.29^{ab}	1.97 ± 0.34^{ab}
1745-81-9	2-propenylphenol	28.331	Spicy, clove-like	1.46 ± 0.41^{a}	0.78 ± 0.28^{ab}	0.47 ± 0.28^{b}	0.19 ± 0.18^{b}
4748-78-1	Benzaldehyde, 4-ethyl-	29.005	Almond, cherry-like	0.57 ± 0.44^{a}	0.11 ± 0.11^{a}	0.31 ± 0.35^{a}	0.31 ± 0.36^{a}
119-36-8	Methyl salicylate	29.42	Wintergreen, minty	1.36 ± 0.29^{a}	0.47 ± 0.16^{b}	0.56 ± 0.17^{b}	0.49 ± 0.29^{b}
623-27-8	1.4-Benzenedicarboxaldehyde	31.024	Not well documented	0.77 ± 0.25^{a}	0.20 ± 0.16^{a}	0.24 ± 0.24^{a}	0.25 ± 0.25^{a}
626-19-7	Isophthalaldehyde	31.261	Slightly sweet, aldehydic	1.09 ± 0.37^{a}	0.22 ± 0.20^{b}	0.50 ± 0.31^{ab}	0.31 ± 0.38^{ab}
104-94-9	p-anisaldehyde	31.832	Sweet, floral, anisic	0.25 ± 0.24^{a}	0.07 ± 0.09^{a}	0.20 ± 0.28^{a}	0.15 ± 0.25a
112-05-0	Nonanoic acid	32.191	Waxy, fatty, rancid	0.25 ± 0.20^{a}	0.26 ± 0.20 ^{a}	0.24 ± 0.30^{a}	0.13 ± 0.21^{a}
6066-49-5	Butyl phthalide-3-N	34.772	Celery-like, herbal	1.04 ± 0.39^{a}	0.22 ± 0.23^{b}	0.28 ± 0.21^{ab}	0.29 ± 0.30^{ab}
637-33-2	Hydrazine, 1-(3-hydroxybenzyl)-	37.467	Not well documented	1.09 ± 0.32^{a}	0.90 ± 0.33^{a}	0.05 ± 0.09^{b}	0.15 ± 0.26^{b}
501-94-0	p-Tyrosol	37.495	Mildly floral, slightly phenolic	1.27 ± 0.35^{a}	1.03 ± 0.24^{a}	0.89 ± 0.41^{a}	1.21 ± 0.30^{a}

RT: retention time. CAS number and odor descriptors from PubChem (https://pubchem.ncbi.nlm.nih.gov/, accessed on 12 March 2025). nd: not detected. Different lowercase letters in the same row indicate statistically significant differences between fermentation times ($p < 0.05$, Tukey's HSD test).

In EVOO, (E)-2-hexenal and (Z)-3-hexen-1-ol (C6-LOX family, fruity–green notes) predominate, whereas in VOO/LOO there are increases in hexanal/nonanal (oxidation) and ethyl acetate/2-

propanol (fermentation/winey–vinegary). Ad-EVOO 25% exhibits an intermediate profile. Figure 3 (bars) illustrates these differences for the most informative markers. This chemical gradient explains the separation in Figure 2 and is consistent with recent reviews on the LOX pathway and the evolution of volatiles during storage [24,25].

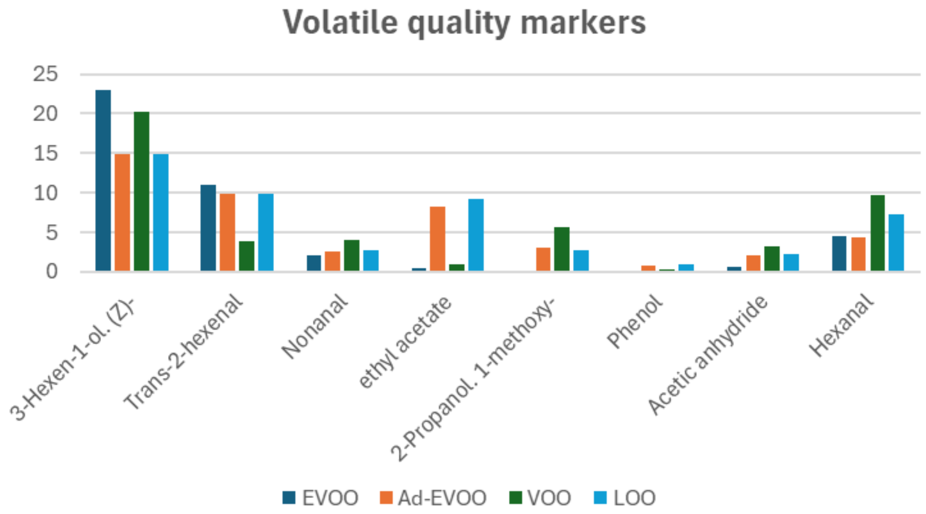

Figure 3. Mean distribution (% area) of C6-LOX volatiles and defect markers by class.

C6-LOX compounds—(Z)-3-hexen-1-ol and (E)-2-hexenal—are highest in EVOO, still elevated in VOO, intermediate in Ad-EVOO 25%, and minimal in LOO, consistent with the fruity–green profile characteristic of the LOX pathway [25]. By contrast, defect markers increase in lower categories: ethyl acetate (fermentation/winey–vinegary) and 1-methoxy-2-propanol are higher in LOO (and, to a lesser extent, in Ad-EVOO 25%) and low or residual in EVOO/VOO, while oxidation aldehydes (hexanal and, to a lesser extent, nonanal) rise in VOO and LOO relative to EVOO/Ad-EVOO, consistent with ageing/oxidation during storage [25]. Fenol y anhídrido acético permanecen en niveles residuales en todas las clases.

Taken together, the “high C6 + low defect markers” pattern characterises EVOO, the opposite pattern characterises VOO/LOO, and Ad-EVOO 25% exhibits an intermediate profile, consistent with its position in the LDA projection [24–26].

3.3. Adulteration AOVE with SFO

Adulteration of EVOO with lower-cost oils, such as SFO, remains one of the most frequent frauds and calls for rapid, portable screening tools to flag and hold suspect lots prior to official confirmation (panel/GC–MS) [27]. MOS-sensor electronic noses have shown sensitivity to discriminate EVOO–SFO blends under field-like conditions, making them suitable candidates for reception and storage lines [22]. With this motivation, we designed a controlled blending gradient (100% EVOO; Ad-EVOO 5, 10, 20, 40%; and 100% SFO) to assess level detection using LDA/ANN-DA and the quantification of %EVOO by PLS. Figure 4 shows the LDA for EVOO–SFO blends (LV1 = 89.49%; LV2 = 9.36%).

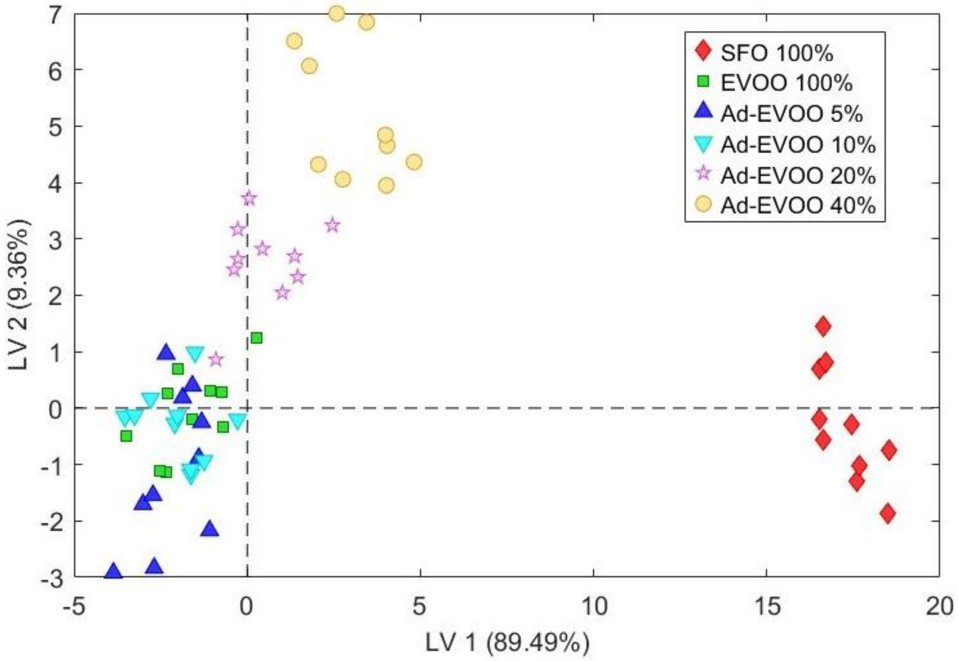

Figure 4. LDA for EVOO–SFO blends (classes: 100% EVOO, 95–60% EVOO, and 100% SFO).

The LV1 axis acts as an SFO gradient: the 100% EVOO cluster concentrates at LV1 < 0 with LV2 near 0, whereas 100% SFO is strongly shifted to LV1 ≫ 0 (≈15–19) with LV2 close to 0, with no overlap with EVOO. Low adulteration levels (Ad-EVOO 5–10%) lie adjacent to the EVOO cluster in the negative LV1 half-plane (LV2 ≈ −1 to 1). From 20% Ad-EVOO onwards, the set forms an intermediate band that crosses LV1 ≈ 0 and rises in LV2 (≈2–3.5), already showing clear separation from EVOO. At 40% Ad-EVOO, the cluster sits in the upper-right quadrant (LV1 ≈ 3–6; high LV2, ≈4–7), well differentiated from both extremes. Overall, the centroids trace a monotonic trajectory—from negative LV1 (EVOO) to highly positive LV1 (SFO)—with a progressive increase in LV2 up to ≈40% SFO and a subsequent decrease in pure SFO; this suggests that LV1 encodes the baseline difference between matrices (EVOO↔SFO), while LV2 captures mixture effects. Operationally, the plot delineates a detection threshold of ≈20% SFO, consistent with reports for portable ENs in oil adulteration and with recent reviews on practical detection limits in EVOO–SFO blends [22,27].

In conclusion, Figure 4 shows that class separation emerges at ≥20% SFO—an operational threshold useful for flagging during screening. Table 4 (ANN-DA) concentrates correct classifications at the extremes (100% SFO and 60–80% EVOO) and shows mild confusions between contiguous levels (95–90% EVOO), a pattern typical of graded problems. Recent studies with portable MOS sensors report convergent results for EVOO–SFO blends, reinforcing the feasibility of compact, field-deployable solutions [22,27].

Table 4. Confusion matrix of the ANN-DA classifier (entries: number of samples).

Real Values	Predicted Values					
	SFO 100%	EVOO 100%	Ad-EVOO 5%	Ad-EVOO 10%	Ad-EVOO 20%	Ad-EVOO 40%
SFO 100%	10	0	0	0	0	0
EVOO 100%	0	8	0	1	0	0
Ad-EVOO 5%	0	0	9	1	0	1
Ad-EVOO 10%	0	2	1	8	1	0
Ad-EVOO 20%	0	0	0	0	9	1
Ad-EVOO 40%	0	0	0	0	0	8

The classifier achieves an overall accuracy of 86.7% (52/60). The error pattern is consistent with a blending gradient: confusions concentrate between contiguous levels (EVOO ↔ 5% ↔ 10% ↔ 20% ↔ 40%), whereas the extremes (100% EVOO and, especially, 100% SFO) show the greatest robustness. Operationally, this supports using the EN as a screening tool with reliable flagging from ~20% SFO (see also the separation in Figure 4), while reserving adjacent cases (around 10%) for confirmatory analysis.

For quantification, the PLS model in Figure 5 was trained on 80% of the 60 samples and evaluated on the remaining 20% in an external validation set.

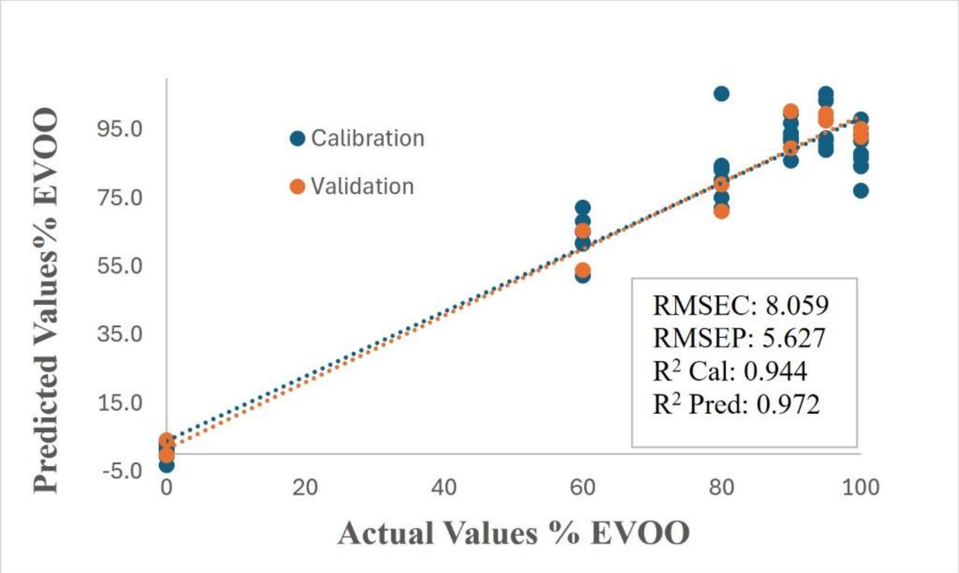

Figure 5. PLS prediction of %EVOO purity.

PLS with an 80/20 external hold-out predicts %EVOO with R²_cal = 0.944 and R²_pred = 0.972; RMSEC/RMSEP = 8.059/5.627. This scheme adheres to good practice for demonstrating generalisation and reducing optimism in multivariate regression. The oil-adulteration literature—using both ENs and sensor fusion (e.g., EN + ultrasound)—supports the use of supervised models to estimate blending gradients [28]. In conclusion, Figure 5 demonstrates predictive capability to estimate %EVOO purity in potential adulteration scenarios (high R²pred and errors compatible with screening), enabling flagging above internal thresholds and prioritisation of confirmatory analyses.

3.4. Limitations, Robustness, and Avenues for Improvement

Drift and T/RH. MOS-based ENs are sensitive to drift and to temperature/relative humidity (T/RH); options include calibration updates, ensembles, and domain adaptation. Literature from 2022–2025 reports significant gains when incorporating drift compensation (e.g., semi-supervised/ensemble approaches) and T/RH covariates. We recommend a model-maintenance plan and multi-site external validations to consolidate the domain of applicability [29–31].

Future lines. (i) Expand sample size and diversity (cultivars, crop years, mills); (ii) evaluate transfer between instruments/campaigns with calibration updates or invariant models; (iii) explore temporal features and ensembles to mitigate drift; (iv) integrate T/RH sensors as covariates; (v) conduct multi-site external validation and blinded studies against the panel/GC–MS to estimate performance under real-world conditions.

This study demonstrates that a MOS-based EN, combined with chemometrics, is an objective, rapid, and non-destructive screening tool for quality control of virgin olive oils and for detecting adulteration with SFO. In classification, LDA separates the three categories (EVOO, VOO, and LOO) plus the adulterated sample (Ad-EVOO 25%), and the ANN-DA classifier reaches 90% accuracy under cross-validation, with errors concentrated in the VOO↔LOO pair, consistent with their olfactory proximity. Per-class metrics show F1 = 1.00 for EVOO and Ad-EVOO 25% and F1 ≈ 0.78–0.86 for VOO/LOO—a pattern reported in recent EN studies on olive oils and portable devices [15,21].

HS-SPME-GC–MS corroboration supports the olfactory separation: higher LOX-pathway C6 volatiles in EVOO and increased oxidation/fermentation markers in VOO/LOO, providing chemical traceability to the instrumental decision. These volatile changes agree with the literature on ageing/rancidity and on cultivar/crop-year variability [24–26].

For EVOO–SFO adulteration, the LDA projection shows separation emerging at ≥20% SFO, an operational threshold suitable for screening flags; ANN-DA concentrates correct classifications at composition extremes with mild confusions between contiguous levels—typical of graded problems. PLS regression with external validation predicts %EVOO with R^2_pred = 0.972 (RMSEC/RMSEP = 8.06/5.63), adequate for prioritising confirmatory analyses when the signal exceeds internal thresholds [22,27,28].

Operationally, we propose using the EN for pre-classification at reception/storage, referring borderline cases (VOO↔LOO, blends <20% SFO or near internal limits) to the panel and/or GC–MS. For robustness in real deployments, we recommend a plan for model maintenance and updates with compensation/transfer strategies against drift, as suggested in recent work (ensemble/semi-supervised/calibration-update approaches) [29–31].

Limitations and future work include increasing n and diversity (cultivars, crop years, mills), multi-site external validation, explicit integration of T/RH covariates, and transfer studies between instruments/campaigns with calibration updates or invariant models. These measures will consolidate the domain of applicability and the reproducibility of the system under real conditions.

Supplementary Materials: The following supporting information will be available online: File S1-Raw EN signals adulteration; File S2- Raw signals category; File S3-Electronic Nose Prototype: System Architecture and Pneumatic Flow Path.

Author Contributions: Conceptualization, R.S.; Methodology, R.S. and F.D.; Software, F.D.; Validation, R.S. and F.D.; Formal analysis, R.S. and F.D.; Investigation, R.S. and L.M.; Resources, R.S.; Data curation, L.M. and R.S.; Writing—original draft preparation, R.S.; Writing—review and editing, R.S., F.D. and L.M.; Visualization, F.D.; Supervision, R.S.; Project administration, R.S.; Funding acquisition, R.S. All authors have read and agreed to the published version of the manuscript.

Funding: This research was funded by the NECA project ("Development of new electronic nose prototypes and analysis with artificial-intelligence neural networks for food quality monitoring"), funded by the Junta de Extremadura. The project is part of the Operational Programme FEDER Extremadura 2021–2027, Action 1A1103 (Development of scientific research, technological development, and innovation capacity), co-financed by the European Regional Development Fund (ERDF) at 85%.

Institutional Review Board Statement: Not applicable.

Informed Consent Statement: Not applicable.

Data Availability Statement: Data is contained within the article and the Supplementary Materials. Additional data is available from the corresponding author on reasonable request.

Acknowledgments: The authors gratefully acknowledge Compañía Oleícola Siglo XXI S.L. (La Chinata, Spain) for providing samples and operational support within the project "Development of new electronic nose prototypes and artificial intelligence-based neural network analysis for food quality monitoring (NECA)", led by CICYTEX. The authors also thank CICYTEX for their institutional support and participation.

Conflicts of Interest: The authors declare no conflict of interest. The funders had no role in the design of the study; in the collection, analyses, or interpretation of data; in the writing of the manuscript; or in the decision to publish the results.

Abbreviations

The following abbreviations are used in this manuscript:

EN	Electronic nose
MOS	Metal-oxide-semiconductor
VOC(s)	Volatile organic compound(s)

LD	Linear dichroism
HS-SPME-GC–MS	Headspace solid-phase microextraction gas chromatography–mass spectrometry
LDA	Linear discriminant analysis
ANN-DA	Artificial neural-network discriminant analysis
PLS	Partial least-squares regression
IOC	International Olive Council
EVOO / VOO / LOO	Extra virgin / Virgin / Lampante olive oil
Ad-EVOO	Adulterated EVOO
SFO	Sunflower oil
Md / Mf	Median of defect / Median of fruitiness
LV(s)	Latent variable(s)
T/RH	Temperature/relative humidity
IAQ	Indoor air quality (IAQ device channel family)
TVOC	Total volatile organic compounds
CO_2eq	Carbon dioxide equivalent (device index)
RMSEC / RMSEP	Root means square error of calibration / prediction
R^2cal / R^2pred	Coefficients of determination (calibration / external prediction)

References

1. International Olive Council (IOC). *Sensory Analysis of Olive Oil—Method for the Organoleptic Assessment of Virgin Olive Oil*, COI/T.20/Doc. No 15/Rev. 11; IOC: Madrid, Spain, 2024.
2. European Union. Commission Delegated Regulation (EU) 2022/2104 of 29 July 2022 supplementing Regulation (EU) No 1308/2013 as regards marketing standards for olive oil (consolidated 10 June 2024). Available online: ELI: 32022R2104. (accessed on 1 September 2025).
3. European Union. Commission Implementing Regulation (EU) 2022/2105 of 29 July 2022 laying down rules on conformity checks of marketing standards for olive oil (consolidated 11 November 2024). Available online: ELI: 32022R2105.
4. Kalua, C.M.; Allen, M.S.; Bedgood, D.R.; Bishop, A.G.; Prenzler, P.D.; Robards, K. Olive oil volatile compounds, flavour development and quality: A critical review. *Food Chem.* **2007**, *100*, 273–286.
5. Angerosa, F.; Servili, M.; Selvaggini, R.; Taticchi, A.; Esposto, S.; Montedoro, G.F. Volatile compounds in virgin olive oil: occurrence and their relationship with the quality. *J. Chromatogr.* **2004**, *1054*, 17–31.
6. International Olive Council (IOC). *Method for the Chromatographic Analysis of Volatile Compounds in Virgin Olive Oils* (HS-SPME-GC-FID/MS), COI/T.20/Doc. No 37; IOC: Madrid, Spain, 2024.
7. Valli, E.; Panni, F.; Casadei, E.; Barbieri, S.; Cevoli, C.; Bendini, A.; García-González, D.L.; Gallina Toschi, T. An HS-GC-IMS method for the quality classification of virgin olive oils as screening support for the Panel Test. *Foods* **2020**, *9*, 657.
8. Gerhardt, N.; Schwolow, S.; Rohn, S.; Pérez-Cacho, P.R.; Galán-Soldevilla, H.; Arce, L.; Weller, P. Quality assessment of olive oils based on temperature-ramped HS-GC-IMS and sensory evaluation: comparison of different processing approaches by LDA, kNN and SVM. *Food Chem.* **2019**, *278*, 720–728.
9. Roy, M.; Yadav, B.K. Electronic nose for detection of food adulteration: a review. *J. Food Sci. Technol.* **2022**, 59, 846.
10. Mildner-Szkudlarz, S.; Jeleń, H.H. Detection of olive oil adulteration with rapeseed and sunflower oils using MOS electronic nose and SPME-MS. *J. Food Quality* **2010,** *33*, 21–41.
11. Stilo, F.; Jiménez-Carvelo, A.M.; Liberto, E.; Bicchi, C.; Reichenbach S.E.; Cuadros-Rodríguez, L.; Cordero, C. Chromatographic Fingerprinting Enables Effective Discrimination and Identitation of High-Quality Italian Extra-Virgin Olive Oils J. Agric. Food Chem. **2021**, *69*, 8874–8889.
12. Sánchez, R.; Lozano, J.; Arroyo, P.; Meléndez, F. Detection of 2,4,6-Trichloroanisole in sparkling wines using a portable E-nose and chemometric tools. *Chemosensors* **2025**, *13*, 178.
13. Poeta, E.; Núñez-Carmona, E.; Sberveglieri, V.; Lozano, J.; Sánchez, R. Monitoring the olfactory evolution of cold-fermented sourdough using an electronic nose. *Chemosensors* **2025**, *13*, 187.

14. Mutz, Y.S.; Maroum, S.M.; Tessaro, L.L.G.; de Oliveira Souza, N.; de Bem, M.M.; Alves, L.S.; Figueiredo, L.P.; do Rosario, D.K.A.; Bernardes, P.C.; Nunes, C.A. Effectiveness of an E-Nose Based on Metal Oxide Semiconductor Sensors for Coffee Quality Assessment. *Chemosensors* **2025**, *13*, 23.
15. Barbieri, S.; Cevoli, C.; Bendini, A.; Quintanilla-Casas, B.; García-González, D.L.; Gallina Toschi, T. Flash Gas Chromatography in Tandem with Chemometrics: A Rapid Screening Tool for Quality Grades of Virgin Olive Oils. *Foods* **2020**, *9*, 862.
16. Grigoletto, I.; Casadei, E.; Panni, F.; Valli, E.; Cevoli, C.; Bendini, A.; García-González, D.L.; Focante, F.; Savino, A. F.; Carpino, S.; Gallina Toschi, T. Screening tools combined with multivariate data analysis to predict or confirm virgin olive oil classification by the Panel test. *Eur. J. Lipid Sci. Technol.* **2024**, *126*, e2300211.
17. Circi, S.; Capitani, D.; Randazzo, A.; Ingallina, C., Mannina, L.; Sobolev, A.P. Panel test and chemical analyses of commercial olive oils: a comparative study. *Chem. Biol. Technol. Agric.* **2017,** *4*, 18.
18. Ortega-Gavilán, F.; García-Mesa, J.A; Marzal-Fernández, J.C.; Moreno-Ballesteros, F.J.; Rodríguez-García, F.P.; González-Casado, A.; Cuadros-Rodríguez, L. Innovative and thorough practice to certify reference materials for sensory defects of olive oil. *Food Chem*. **2022**, 380, 132195.
19. Teixeira, G.G.; Dias, L.G.; Rodrigues, N.; Marx, I.M.G.; Veloso, A.C.A.; Pereira, J.A.; Peres, A.M. Application of a Lab-Made Electronic Nose for Extra Virgin Olive Oils Commercial Classification According to the Perceived Fruitiness Intensity. Talanta 2021, 226, 122122. doi:10.1016/j.talanta.2021.122122.
20. Chacón, I.; Roales, J.; Lopes-Costa, T.; Pedrosa, J.M. Analyzing the Organoleptic Quality of Commercial Extra Virgin Olive Oils: IOC Recognized Panel Tests vs. Electronic Nose. *Foods* **2022**, *11*, 1477
21. Amini, A.; Anjileh, H.G.; Amirfaridi, H. Fast and portable single-sensor electronic nose for accurate quality assessment of extra virgin olive oil using a temperature-modulated generic gas sensor. *Talanta* **2026**, 296, 128490.
22. Parlak, İ.H., Milli, M. & Milli, N.S. Machine Learning–Based Detection of Olive Oil Adulteration Using BME688 Gas Sensor Matrix. *Food Anal. Methods* **2025**, 18, 1454–1464.
23. Liu, T.; Guo, L.; Wang, M.; Su, C.; Wang, D.; Dong, H.; Chen, J.; Wu, W. Review on algorithm design in electronic noses: challenges, status, and trends. *Intell. Comput.* **2023**, *2*, 0012.
24. Soldo, B.; Jukić Špika, M.; Pasković, I.; Vuko, E.; Polić Pasković, M.; Ljubenkov, I. The Composition of Volatiles and the Role of Non-Traditional LOX on Target Metabolites in Virgin Olive Oil from Autochthonous Dalmatian Cultivars. *Molecules* **2024**, *29*, 1696.
25. Tucci, R.; Cevoli, C.; Bendini, A.; Barbieri, S.; Casadei, E.; Valli, E.; Gallina Toschi, T. Changes in the Volatile Profile, Fruity Flavor, and Rancidity in Virgin Olive Oils During Storage by Targeted and Untargeted Analytical Approaches. *Foods* **2025**, *14*, 1884.
26. Tomé-Rodríguez, S.; Ledesma-Escobar, C.A.; Penco-Valenzuela, J.M.; Priego-Capote, F. Cultivar influence on the volatile components of olive oil formed in the lipoxygenase pathway. *LWT* **2021**, *147*, 111485.
27. Hashempour-Baltork, F.; Vali Zade, S.; Mazaheri, Y.; Mirza Alizadeh, A.; Rastegar, H.; Abdian, Z.; Torbati, M.; Azadmard-Damirchi, S. Recent methods in detection of olive oil adulteration: state-of-the-art. *J. Agric. Food Res*. **2024**, *16*, 101123.
28. Zarezadeh, M.R.; Aboonajmi, M.; Ghasemi-Varnamkhasti, M. The effect of data fusion on improving the accuracy of olive oil quality measurement. *Food Chem*. X **2023**, *18*, 100622.
29. Jiang, K.; Zeng, M.; Wang, T.; Wu, Y.; Ni, W.; Chen, L.; Yang, J.; Hu, N.; Zhang, B.; Xuan, F.; Li, S.; Shi, A.; Yang, Z. Gas sensor drift compensation using semi-supervised ensemble classifiers with multi-level features and center loss. *ACS Sens.* **2025**, *10*, 2906–2918.
30. Fan, H.; Schaffernicht, E.; Lilienthal, A.J. Ensemble learning-based approach for gas detection using an electronic nose in robotic applications. *Front. Chem.* **2022**, *10*, 863838.
31. Rudnitskaya, A. Calibration update and drift correction for electronic noses and tongues. *Front. Chem.* **2018**, *6*, 433.